

Nanosized Particles of X Zeolite Containing Ammonium Cations as Basic Catalysts

João G. P. Vicente¹ · Patrícia M. Lima¹ · Dilson Cardoso¹

Received: 22 October 2016 / Accepted: 2 January 2017 / Published online: 15 February 2017
© Springer Science+Business Media New York 2017

Abstract There is great interest in reducing the size of zeolite particles, because this can improve their catalytic properties in various reactions. This work evaluates two faujasite-type X zeolites, one micrometric and one nanometric. Zeolites in the sodium form were exchanged ionically with methylammonium cations. The materials were then evaluated as catalysts in the Knoevenagel condensation reaction. Steric impediments restricted ion exchange in the micrometric zeolite and became more important with increasing cation volume. In the case of the nanometric sample, such impediments were less evident, because the smaller particle size provided greater access of exchanger cations, compared to the micrometric zeolite in which the sodium was inaccessible. The best catalytic performances were achieved with zeolites containing the monomethylammonium cation. The increased accessibility and diffusion of

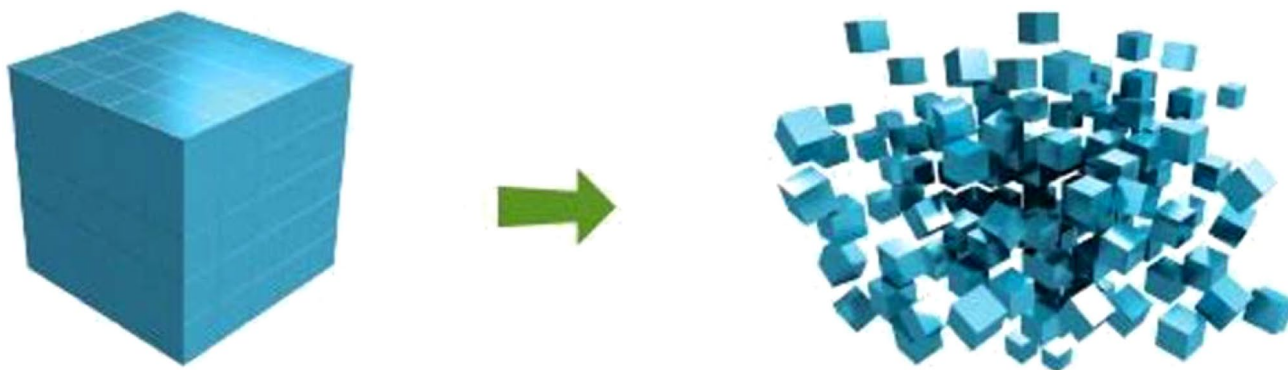
the reactants and products through the pores of the nanometric zeolite provided the best butyraldehyde conversions, independent of the exchanger cation. In order to increase accessibility to catalytic sites, several studies have been carried out in order to reduce the diameter of the particles of zeolites to the nanometer scale. This reduction can promote the increase in the activity of the catalysts in some reactions.

Graphical Abstract In order to increase accessibility to catalytic sites, several studies have been carried out in order to reduce the diameter of the particles of zeolites to the nanometer scale. This reduction can promote the increase in the activity of the catalysts in some reactions.

Electronic supplementary material The online version of this article (doi:10.1007/s10562-017-1969-9) contains supplementary material, which is available to authorized users.

✉ Dilson Cardoso
dilson@ufscar.br

¹ Catalysis Laboratory, Chemical Engineering Department, Federal University of São Carlos, P.O. Box 676, São Carlos 13565-905, Brazil



Keywords X zeolite · Nanoparticles · Ion exchange · Basic catalysis · Knoevenagel condensation · Turnover frequency (TOF)

1 Introduction

There is increasing interest in reducing the size of zeolite particles from the micrometric to the nanometric scale [1–3]. This modification significantly alters the properties of zeolites, mainly due to increases in the external area and greater access to catalytic sites [4]. This results in different performance, even in traditional applications such as separation and catalysis [1, 5].

Despite their great potential for use in industrially important reactions, there have been only a few studies of the use of microporous molecular sieves with basic properties in reactions such as the Claisen, Knoevenagel, aldol, and transesterification condensations. At present, considering all industrial applications of acid, base, and bifunctional solid catalysts, only 8% of the processes are catalyzed by materials with basic properties [6].

The basicity of zeolites is related to the oxygen anions present in their networks. The basic sites are associated with structural oxygen atoms located close to the charge compensating cations [7]. These oxygen anions are generated by the insertion of aluminum atoms into the zeolite network, and the number of basic sites is equal to the number of aluminum atoms in the structure. The structural aluminum concentration not only affects the charge distribution, but also the number of basic sites present in the zeolite. The strength of these sites mainly depends on the acidity of the charge compensating cation, as well as the aluminum content in the zeolite network [7, 8].

Ion exchange in zeolites involves cations that compensate the negative charges of the structural $[\text{AlO}_4]^-$ tetrahedrals [4, 7]. Studies of such processes have been performed using types X and Y faujasite zeolites exchanged with

methylammonium cations containing different numbers of methyl groups [9–13]. In the Knoevenagel condensation, X zeolite provides higher conversions than Y zeolite, independent of the methylammonium cation used to compensate the negative charge. This is because the network of X zeolite has a greater aluminum content, which increases the number and strength of sites with basic properties [11–13].

The aim of this work was to determine the influence of the size of faujasite zeolite particles containing ammonium cations with different methyl groups on the properties of the material. Catalytic evaluation was performed using the Knoevenagel condensation reaction.

2 Experimental

2.1 Synthesis of Nanometric X Zeolite

The reagents used in the synthesis were Aerosil 380 (Evonik) as Si source, sodium aluminate (Riedel de Haen; 54% Al_2O_3 : 41% Na_2O : 5% H_2O) as Al source, sodium hydroxide (Quimis) as mineralizing agent, and deionized water.

The synthesis of the nanometric faujasite (FAU) zeolite was based on the experimental procedure described in the literature, using the molar ratio: $8.5\text{Na}_2\text{O}:1.0\text{Al}_2\text{O}_3:10\text{SiO}_2:180\text{H}_2\text{O}$ [3]. The required quantities of sodium aluminate and sodium hydroxide were dissolved in a suitable volume of water. The silica was then added, under agitation, until a homogeneous reaction mixture was obtained. The mixture was placed in a thermostatic bath for a determined crystallization period (24, 48, or 72 h), at temperatures of 25, 40, 50, 60, or 70 °C. These temperatures were lower than used in traditional synthesis (100 °C), [3] so the procedure was termed a “mild crystallization”. The precipitate was then centrifuged and washed repeatedly with deionized water until pH 8. The solid was dried in an oven at 60 °C for 12 h.

2.2 Preparation of the Catalysts

The catalysts were prepared using two precursors: the synthesized nanometric zeolite (N-NaX) and a commercial micrometric zeolite (NaX, Aldrich). The sodium cations in the zeolites were replaced with methylammonium cations by ionic exchange [14, 15]. The following nomenclature was used to identify the ammonium cations: Me_i^+ , where i represents the number of methyl groups. The ammonium cations were used in the form of the chlorides, obtained as follows: $i=0$ (purity $\geq 99.5\%$, Aldrich), $i=1$ (purity $> 98\%$, Acros Organics), $i=3$ (purity $> 97\%$, Fluka), and $i=4$ (purity $> 97\%$, Aldrich). Table 1 shows the nomenclature of the catalysts, according to the type of cation and zeolite.

In order to obtain samples with the maximum degree of exchange, three consecutive exchanges were performed using a system under constant agitation at 40°C , to which was added 2 g of the zeolite. Each reaction used an ion exchange solution with a concentration of 0.05 mol L^{-1} .

2.3 Characterization

The zeolites were characterized by means of X-ray diffraction, using a Rigaku Multiflex diffractometer with a Cu tube and Ni filter, operated with $\text{CuK}\alpha$ radiation ($\lambda=0.1542\text{ nm}$), scanning from 2θ of 5° to 35° at a rate of 2° min^{-1} , in steps of 0.02° . The width at half height was determined for the three most intense peaks at 2θ of 15° (331), 23° (533), and 27° (642), using metallic Si as a reference to correct the peak width. The Scherrer equation was used to calculate the crystal diameter in each of the hkl planes (Eq. 1).

$$D_{hkl}(nm) = \frac{K \cdot \lambda}{\beta \cdot \cos \theta} \quad (1)$$

where:

D_{hkl} = Average diameter;

K = Constant (0.94, assuming spherical particles);

λ = Wavelength of the X-ray source;

θ = Bragg angle of the diffraction plane;

$\beta = [(L_{\text{OBS}})^2 - (L_{\text{PAD}})^2]$ (empirical parameter used to correct for experimental errors);

Table 1 Cations and nomenclature used

| Cation | Zeolite | |
|------------------------------|-----------------------|--------------------|
| | Micrometric | Nanometric |
| Na^+ | Na X | N-Na X |
| NH_4^+ | Me_0X | N- Me_0 X |
| CH_3NH_3^+ | Me_1X | N- Me_1 X |
| $(\text{CH}_3)_3\text{NH}^+$ | Me_3X | N- Me_3 X |
| $(\text{CH}_3)_4\text{N}^+$ | Me_4X | N- Me_4 X |

L_{OBS} = Width at half height of the sample diffraction peak;

L_{PAD} = Width at half height of the most intense diffraction peak of the metallic silicon (external standard).

The intensities of the peaks described above were used to calculate the relative crystallinities of the samples, using the high crystallinity NaX sample ($\text{Si}/\text{Al}=1.4$) supplied by Aldrich as a standard. The diameters of the crystals and the crystallinity values were calculated as the averages of three determinations.

Nitrogen physisorption measurements were performed at the boiling temperature of liquid nitrogen (-196°C), using a Micromeritics ASAP-2020 instrument. Adsorbed water was eliminated by pretreating the samples under vacuum at 200°C for 2 h. The volume of micropores (V_{micro}) and the external area (A_{ext}) were determined using the t-plot method [16].

Particle shape and dimensions were examined using scanning electron microscopy (SEM) (Magellan 400 L, FEI). The average diameter of the nanometric zeolite (N-NaX) was estimated by analyzing around 100 particles in various micrographs.

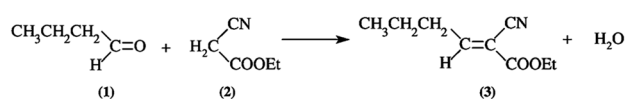
2.4 Ion Exchange

The concentrations of sodium and aluminum in the samples were determined by energy dispersive spectroscopy (EDS) and inductively coupled plasma atomic emission spectroscopy (ICP-OES).

Thermogravimetric analyses were performed using a TA Instruments Model SDT Q600 analyzer, with heating to 800°C at a rate of $10^\circ\text{C min}^{-1}$, under a flow of N_2 (40 mL min^{-1}).

X-ray photoelectron spectroscopy (XPS) analyses were performed using a VSW HA-100 spherical analyzer, equipped with an $\text{AlK}\alpha$ source ($h\nu=1486.6\text{ eV}$), at a pressure less than 10^{-8} mbar. The loading effects were adjusted by linear displacement of the spectrum, so that the C1s signal had a binding energy equal to 284.6 eV . The high-resolution spectra were obtained with constant pass energy of 44 eV , which produced a half width of 1.8 eV for the Au 4f7/2 line.

Evaluation of catalytic activity employed the Knoevenagel condensation (Scheme 1). Toluene was used as solvent in an equimolar mixture containing 2.4 mmol butyraldehyde (Compound 1) and ethyl cyanoacetate (Compound 2), to which was added the catalyst (3% by weight, based on the total weight of reactants). The reaction was performed for 1 h at 50°C , under constant magnetic agitation. The reaction product (Compound 3) was analyzed by gas chromatography using a Shimadzu Model GC 2010 gas chromatograph equipped with a flame ionization detector (FID) and an RTX-1 capillary column.



Scheme 1 Knoevenagel condensation

The stability of the catalysts was determined by means of their reuse, under the standard reaction conditions described above. After each reaction, the catalysts were washed with acetone and then dried in an oven at 60 °C. Equation 2 was used to evaluate and compare the catalytic stabilities of the catalysts.

$$\text{Catalytic stability (\%)} = \frac{\text{Yield}_{4 \text{ use}}}{\text{Yield}_{1 \text{ use}}} \cdot 100 \quad (2)$$

Under the reaction conditions employed, the Knoevenagel condensation was always 100% selective towards Compound 3 (Scheme 1).

The turnover frequencies (TOF) of the catalysts were determined at the start of the reactions ($t=0$). The Knoevenagel condensation was performed under the same conditions as described above, with determination of the conversion as a function of time, every 5 min during 1 h. An exponential curve was adjusted to the points, and the initial reaction rate was obtained by derivation of the curve at zero reaction time.

The synthesis of zeolites and catalytic evaluation were performed in triplicate, in order to verify the reproducibility of the results. Thus, the results presented below refer to the average value and the standard deviation (error bar) calculated.

3 Results and Discussion

3.1 Synthesis

The diffractograms shown in Fig. 1 illustrate the influences of temperature and crystallization time on the synthesis of the nanometric FAU zeolite. The samples with evidence of crystallinity presented diffraction peaks corresponding to the faujasite structure, according to comparisons with the commercial NaX sample (Fig. 3). At lower crystallization temperatures (25 and 40 °C), the treatment times were insufficient to obtain a crystalline product, and the diffractograms were characteristic of materials with low degrees of organization. However, with increase of the temperature to 50 °C and using times of 48 and 72 h, there was the formation of a material with sufficient diffraction planes for the appearance of the characteristic zeolite peaks, with no significant differences between the diffractograms.

When the temperature was increased to 60 °C, all the samples showed diffraction patterns indicative of varying degrees of crystallinity, with the peaks becoming narrower and more intense for longer treatment periods.

In the diffractograms for the samples crystallized at 70 °C, the peaks became increasingly narrow and intense with crystallization time, as well as in comparison with the samples crystallized at lower temperatures, which was indicative of crystal growth. In order to confirm this, and to identify the condition that provided the maximum rate of nucleation, while minimizing the effects of crystal growth (hence producing crystals with small diameters), a graph was constructed of relative crystallinity plotted as a function of average crystal diameter (Figure S.1).

There was relationship between crystal diameter and the degree of crystallinity. Both the time and the temperature directly influenced crystallization and the size of the crystals, hence leading to significant differences in terms of the level of organization of the material. The samples obtained with aging for 48 h showed increases of around 5% in crystallinity, and 8 nm in average crystal size, for each 10 °C increase in temperature. The increments were even greater for samples aged for 24 h, with the crystallites obtained at 60 °C showing an average diameter of around 12 nm, while diameters in the region of 30 nm were obtained at 70 °C.

The data obtained using longer crystallization times (48 and 72 h) and higher temperature (70 °C) indicated that equilibrium crystallinity and average diameter could have been reached, since the values of these parameters remained fairly constant. Hence, increase in temperature led to greater total energy of the system, which increased the rates of nucleation and crystallization (using short synthesis times), while at high treatment temperatures, the quantity of nuclei formed was considerably lower, resulting in the growth of crystals [2, 17]. It was therefore important to interrupt the crystallization step before crystal growth became predominant [3, 18, 19]. The morphologies and average diameters of the particles of the samples that exhibited crystallinity are shown in Figure S.2.

The particles obtained using treatment at 50 °C presented approximately spherical morphology, with average diameters around 180 nm. For temperatures of 60 and 70 °C, the particle morphology was irregular, with the formation of polycrystalline plates with average thickness of 40 nm. The dimensions of the particles increased with time, with values of approximately 300 and 500 nm for crystallization at 60 °C for 24 and 72 h, respectively. At 70 °C, equilibrium was reached in terms of particle size and crystal diameter, with sizes of around 800 nm obtained for all aging times. A higher temperature therefore led to particle aggregation and the formation of larger particles [18, 20].

Use of the different temperatures and crystallization times resulted in the formation of faujasite zeolites with

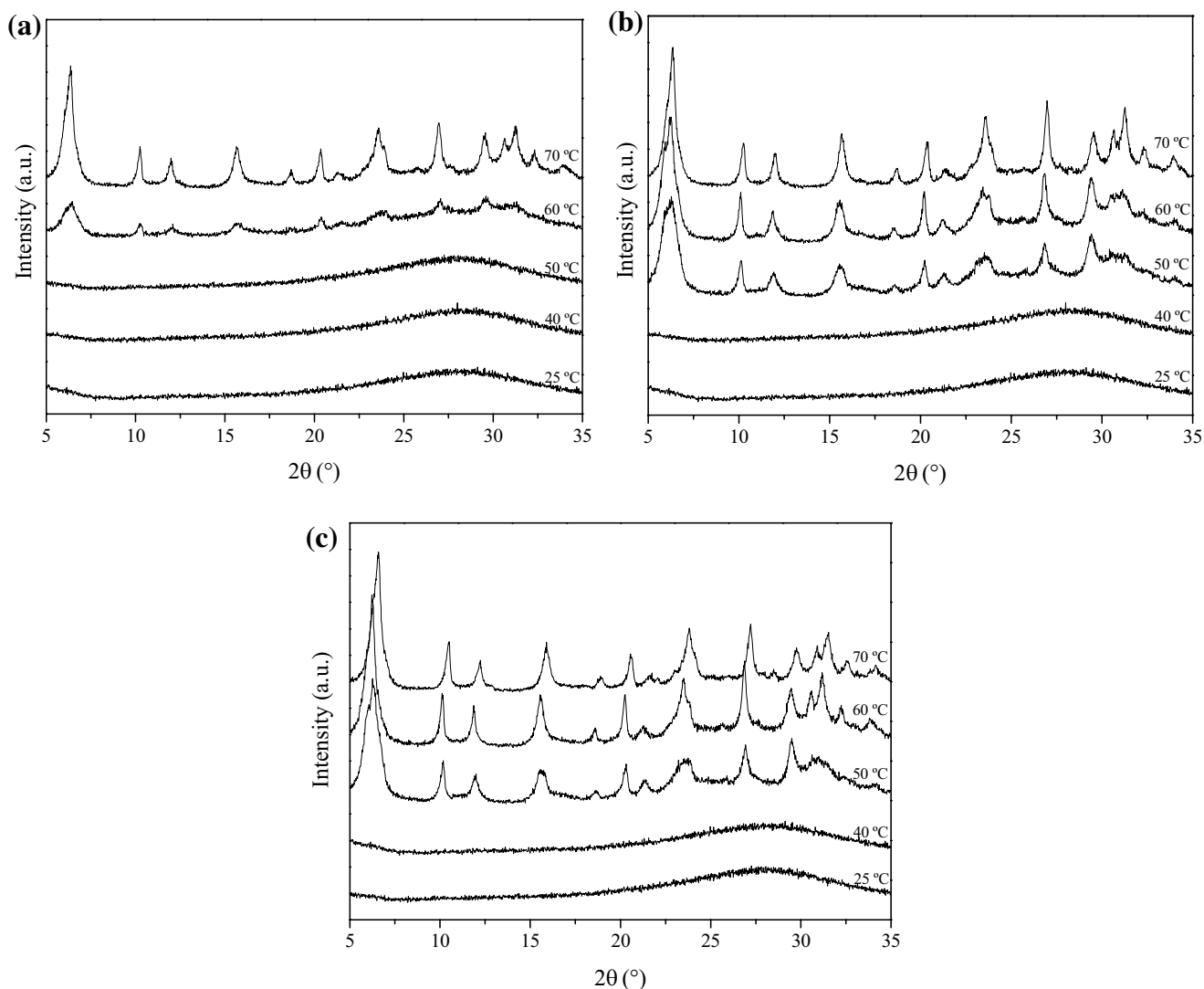


Fig. 1 Diffractograms of samples synthesized using crystallization times of **a** 24, **b** 48, and **c** 72 h, and temperatures of 25, 40, 50, 60, and 70 °C

crystals showing average diameters ranging from 12 to 35 nm and particles with sizes from 170 to 900 nm. A rapid method was therefore required to compare all the synthesized materials and identify the zeolite with the best potential for use in base catalysis.

The catalytic activities of the synthesized materials were evaluated using the Knoevenagel condensation as a model reaction. The samples were in the sodium form, which is associated with low zeolite basicity,[21, 22] so the reaction was performed for a period of 3 h, instead of 1 h as described in Section Sect. 2.4. Figure 2 shows the catalytic conversion of butyraldehyde as a function of the average diameter of the crystals and particles. It can be seen that the sizes of the crystals and particles had a substantial influence on catalyst activity, in agreement with the literature, [2, 3, 23] with the best conversion results obtained using the catalysts with the smallest dimensions. Based on the

catalytic activity results, the *zeolite selected* was the material synthesized using crystallization of the reaction mixture at 60 °C for 24 h to be the precursor material (*micro-sized zeolite*) in continuity of the research.

3.2 Comparison of Precursors

In order to identify the main differences between the zeolites used in this work, it was important to perform a comparison of the initial properties of the two sodic zeolites with FAU structures: N-NaX (composed of nanometric particles) and NaX (composed of micrometric particles), which would be used as catalysts in the subsequent experiments.

Figure 3 shows two distinct diffraction profiles, one characteristic of micrometric FAU zeolite (NaX), with intense narrow peaks reflecting the high degree of organization of

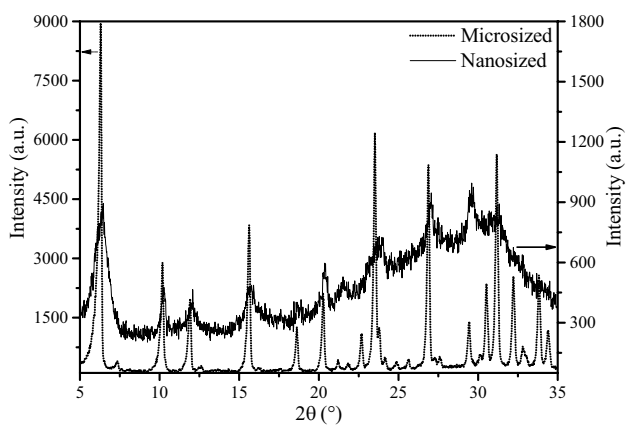


Fig. 2 Conversion of butyraldehyde as a function of crystallite (a) and particle (b) diameter, using zeolites synthesized in the sodium form as catalysts (3 h, 50°C and 3% w/w catalyst)

the material, and another characteristic of nanometric materials, with broader and less intense diffraction peaks [2, 3].

Figure 4 shows micrographs of the two zeolites, revealing distinctly different morphologies. The N-NaX nanometric zeolite consisted of irregular particles with dimensions of around 300 nm, composed of clusters of crystals with average diameter of around 12 nm. In contrast, the NaX zeolite consisted of particles with sizes between 1 and 2 μm and crystals around 80 nm in size.

The nitrogen physisorption isotherms of the zeolites (Fig. 5) showed typical Type 1 BET profiles, characteristic of microporous solids that present high adsorption capacities at low relative pressures. Due to the irregularities associated with the nanometric dimensions of the N-NaX

zeolite, it showed a nitrogen adsorption capacity around threefold lower than obtained with the micrometric sample (up to $P/P_0 = 0.9$).

At the end of the isotherms ($P/P_0 \sim 1$), the zeolites showed nearly the same volumes of adsorbed nitrogen, but in this region, the nanometric material presented an abrupt increase in adsorption capacity. This was indicative of substantial inter-particle porosity (formed between the particles), which was not observed for the micrometric zeolite. Using the BJH method (Figure S.3), and according to the IUPAC classification, the diameter of the pores in nanosized zeolite were in the macropore range, reaching values up to 140 nm. This type of porosity makes an important contribution to mass transfer between the solid particles, especially when it is caused by particles with different diameters, as can be seen in Fig. 5. When the material is porous, as with zeolites, smaller particle diameter decreases the diffusive step, which is the path followed by the molecules in the interiors of the pores. This facilitates the entry of reagents and exit of products during reactions [2].

Application of the t-plot method with the isotherms of Fig. 5 resulted in volumes of micropores of 0.296 and 0.081 cm³ g⁻¹ for the samples with micrometric (NaX) and nanometric (N-NaX) particles, respectively [16]. In terms of the volume of micropores, the nanometric zeolite particles therefore had a relative microporosity of 27%, compared to the micrometric material. These values agreed with the XRD results, where the nanometric sample showed a relative crystallinity of 15%, indicative of a low degree of organization in a material that was still in the formation phase. The t-plot method also enabled determination of the

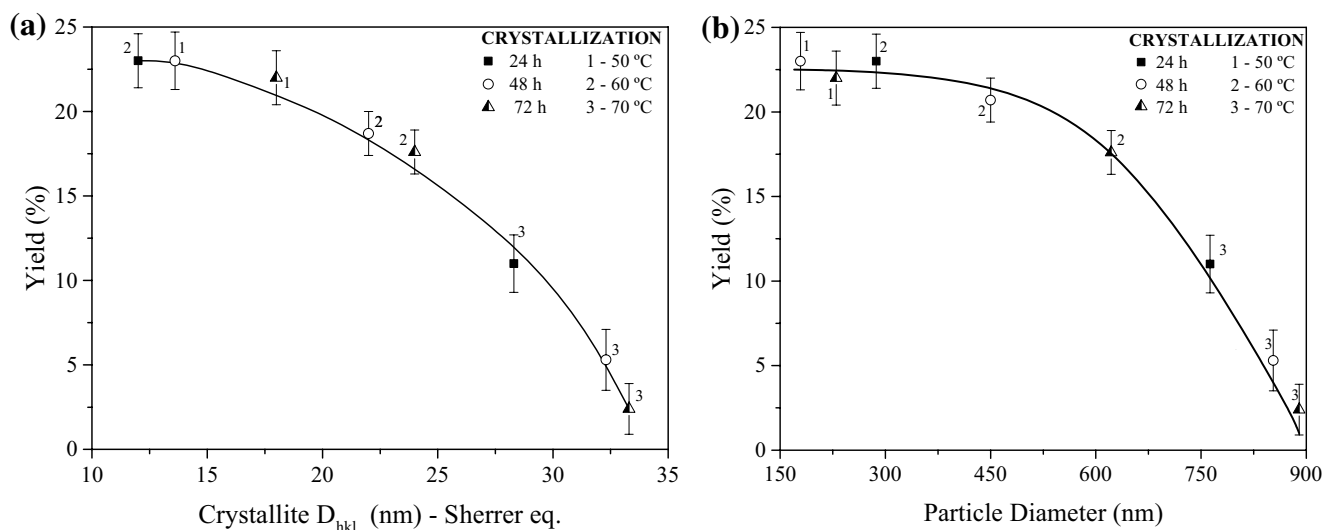


Fig. 3 Diffractograms of nanometric (N-NaX) and micrometric (NaX) zeolites

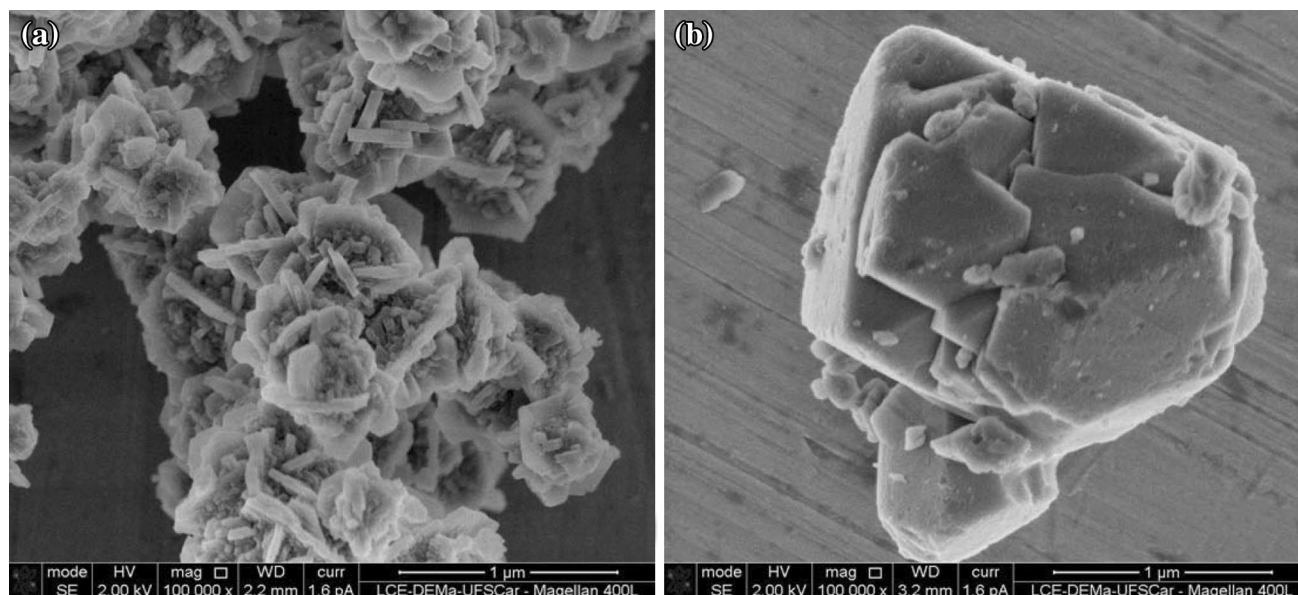


Fig. 4 SEM micrographs of the nanometric (a) and micrometric (b) zeolites

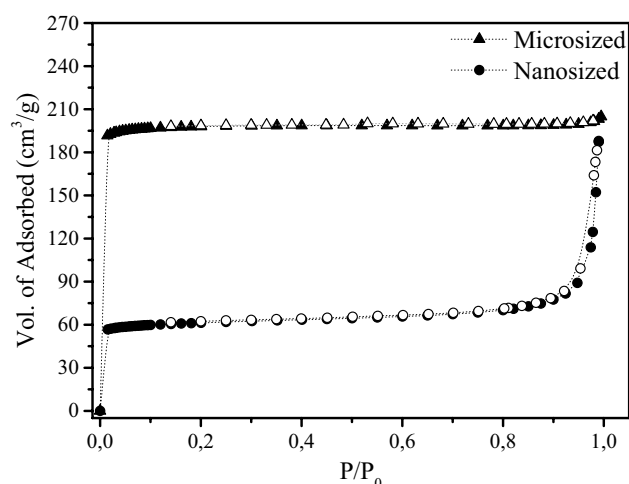


Fig. 5 Nitrogen physisorption isotherms of the NaX and N-NaX zeolites

external areas of the particles, resulting, as expected, in a greater area for the solid with the smallest particles, with values of 33 (N-NaX) and 23 m² g⁻¹ (NaX).

Table 2 provides the values of the main properties of the nanometric and micrometric zeolites, including chemical composition (Si/Al ratio). The two materials presented very similar compositions, with Si/Al values below 1.5, enabling them to be classified as type X faujasites. The materials differed completely in their other properties, especially in terms of the sizes of the crystals and particles. It was therefore necessary to determine the influence of these parameters during the catalytic activity assays.

3.3 Ionic Exchange

According to Breck [24] the sodium cations in the X zeolite structure are distributed into three kinds of crystallographic sites (I, II, and III). The I sites (19%) are located in the interior of the hexagonal prisms that interconnect the sodalites; the II sites (37%), belonging to the hexagonal face of the sodalite, and the III sites (43%), near the square face, are both associated with the supercavity. The radii of the access pores of the sodalite cavities and the hexagonal prisms are approximately 0.11 nm. This value is smaller than the ionic radii of the exchanger cations (dehydrated and hydrated) (Table 3), so due to these restrictions, ion exchange in the X zeolite is restricted to sites located in the supercavity [13, 25, 26]. Therefore, in X zeolite, the ion exchange process is restricted to a maximum value of 81%, because it is impossible to access the I sites.

Figure 6 shows the degrees of ion exchange (D_{iex} %) reached for the nanometric and micrometric zeolites using the cations ammonium (Me_0^+), monomethylammonium (Me_1^+), trimethylammonium (Me_3^+), and tetramethylammonium (Me_4^+). These results were calculated by the Eq. 3 and the values represent the maximum degree of exchange for each of cations, since they were obtained using three successive exchanges.

$$D_{iex}(\%) = \left(1 - \frac{C_{Na}}{22,29} \times \frac{26,96}{C_{Al}} \right) \times 100 \quad (3)$$

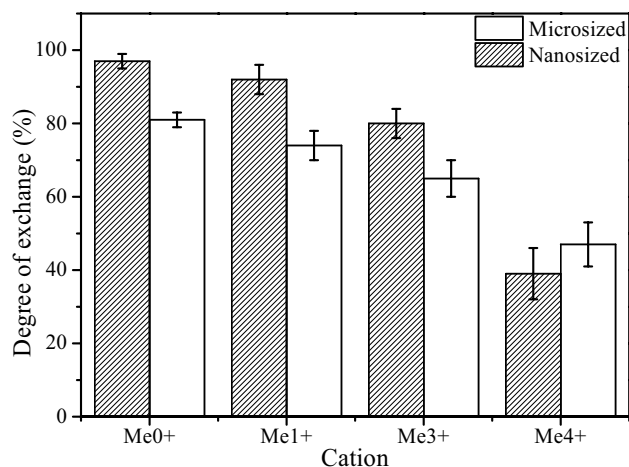
where: C_{Na} e C_{Al} represent the average concentrations of sodium and aluminum (g.ml⁻¹) obtained by the two characterization techniques (ICP, in duplicate; EDS, in triplicate).

Table 2 Main properties of the micrometric and nanometric zeolites

| Parameter | Zeolite | |
|--|-------------|------------|
| | Micrometric | Nanometric |
| Relative crystallinity (%) ^a | 100 | 15 |
| D_{hkl} (nm) ^b | 80 | 12 |
| Volume of micropores (cm ³ g ⁻¹) ^c | 0.296 | 0.081 |
| External area (m ² g ⁻¹) ^c | 23 | 33 |
| V_{micro} (%) ^d | 100 | 27 |
| V_{inter} (cm ³ g ⁻¹) ^e | 0.021 | 0.209 |
| Si/Al ^f | 1.35 | 1.33 |

^aCalculated using XRD^bAverage crystal diameter calculated using the Scherrer equation^cDetermined by the t-plot method^dCalculated using the micrometric sample as standard^e $V_{interparticular} = (V_{(P/P0)} - 0.98) - V_{micro}$ ^fObtained by EDS**Table 3** Ionic radii of the sodium and methylammonium cations (not hydrated and hydrated). [12, 25, 26, 25, 26]

| Cation | Ionic radius (nm) | Hydrated ionic radius (nm) |
|----------|-------------------|----------------------------|
| Na^+ | 0.095 | 0.358 |
| Me_0^+ | 0.148 | 0.331 |
| Me_1^+ | 0.245 | – |
| Me_3^+ | 0.320 | – |
| Me_4^+ | 0.347 | 0.367 |

**Fig. 6** Maximum degrees of ion exchange obtained with the nano-metric and micrometric zeolites

The micrometric zeolite showed degrees of ion exchange below 81% for all the cations, due to the hindrance described above. However, the nanometric FAU

zeolite presented degrees of exchange exceeding 81% for the Me_0^+ and Me_1^+ cations, which has not been previously reported in the literature. An explanation for this behavior can be found in the data shown in Table 2, indicating that the nanometric zeolite possessed low levels of crystallinity and microporosity, characteristic of a material that was still in the process of formation. It is therefore possible that the small cavities that restricted ion exchange had not been fully formed, enabling the exchanger cations to substitute the sodium ions present in the type I sites.

As shown in Fig. 6, for both zeolites, the order of degree of exchange was: $Me_0^+ > Me_1^+ > Me_3^+ > Me_4^+$. It can be seen that none of the exchanger cations could completely substitute the sodium cations present in the zeolites. The sequence obtained was due, at least in part, to the different affinities of the cations for the aluminate anions of the network, as observed for the zeolite with the lowest aluminum content (the Y faujasite), in which the aluminate anions were separated to a greater extent [9]. Furthermore, ion exchange in X faujasite becomes limited by the short distance between the exchangeable sites, hindering accommodation of the cations [9–13]. Figure 6 shows that as the cation diameter increased, the maximum degrees of exchange of the nanometric and micrometric zeolites decreased from approximately 97 to 40%, and from 80 to 45%, respectively.

3.4 Thermogravimetric Analysis (TGA)

Figure 7 shows the thermograms and the corresponding derivative curves for the micrometric and nanometric zeolites. Between 25 and 400 °C, there was weight loss associated with the elimination of physisorbed water from the pores and the dehydration of sodium cations. Around 3% more water was removed from the NaX zeolite, due to the higher volume of micropores in the commercial zeolite.

The derivative curves showed two peaks: a small peak at about 60 °C, related to the desorption of water with low interaction with the cations, and a peak corresponding to the loss of water occluded in the zeolite cavities, which appeared at 120 and 140 °C for the nanometric and commercial zeolites, respectively. These results demonstrated that the nanometric size and irregular morphology of the synthesized zeolite facilitated the process of water desorption, so that lower temperatures were required.

Figure 8 presents the thermograms and derivative curves obtained in an oxidizing atmosphere for the nanometric and micrometric FAU zeolites containing organic cations. The thermograms can be divided into three regions: [26].

Region I: Between 25 and 200 °C, corresponding to desorption of physisorbed water. In general, the temperatures at which the maximum desorption rate occurred

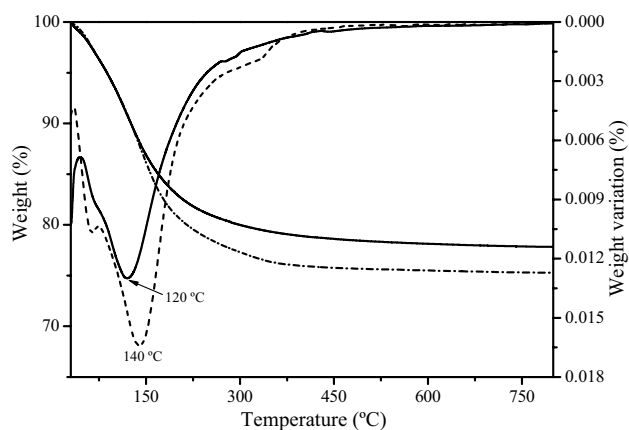


Fig. 7 Thermograms and derivative curves for the micrometric and nanometric zeolites

were lower for the nanometric zeolite, suggesting that the process was facilitated by smaller particle size.

Region II: Between 200 and 550 °C, corresponding to decomposition of the ammonium cations, Me_i^+ . In this region, the definition of the derivative curve peaks improved with increasing amounts of ammonium cations.

Region III: Above 550 °C, weight loss was due to dehydroxylation of the hydroxyl formed by the proton resulting

from decomposition of the methylammonium cations [26–28].

Figure 9 shows the results for water loss from the micrometric and nanometric zeolites containing methylammonium cations, in the temperature range between 25 and 200 °C. In order to relate the amounts of water and organic cations in the structures of the zeolites, the mass losses were expressed in mols.

The degree of hydration of the cations decreased as a function of their volume, so their hydrophobicity also increased, leading to smaller amounts of water present in the zeolite cavities [9]. There was a significantly lower water loss from the Me_1^+ cations, compared to Me_0^+ , due to the greater volume of the exchanger cation, while there were no substantial differences between Me_3^+ and Me_4^+ , in terms of molar water loss.

The samples containing crystals around 12 nm in size showed smaller amounts of water, irrespective of the exchanger cation, while the nanometric and commercial materials presented similar profiles. As described previously, this was because the nanometric zeolite had a smaller volume of micropores and consequently a smaller amount of physisorbed water in its structure.

Table 4 gives the organic cation contents of the zeolites (in mol per 100 g of zeolite), determined from the

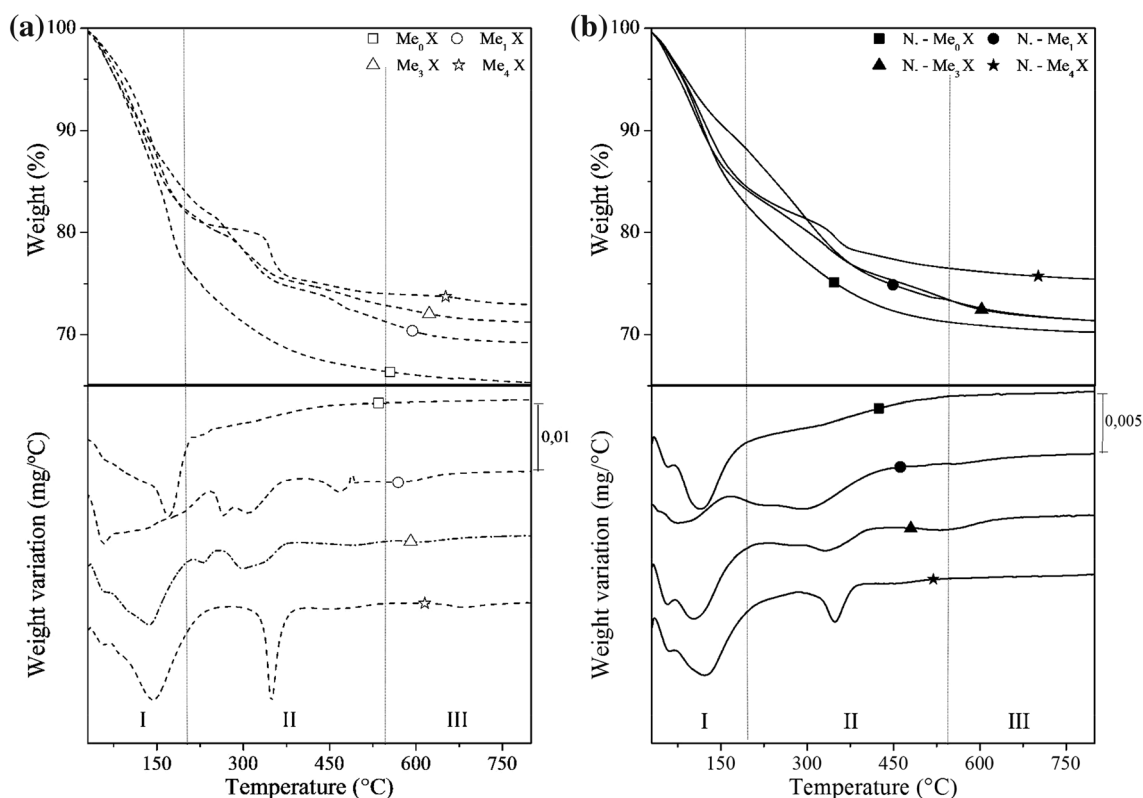


Fig. 8 Thermograms and derivatives for the nanometric (a) and micrometric (b) zeolites containing organic cations

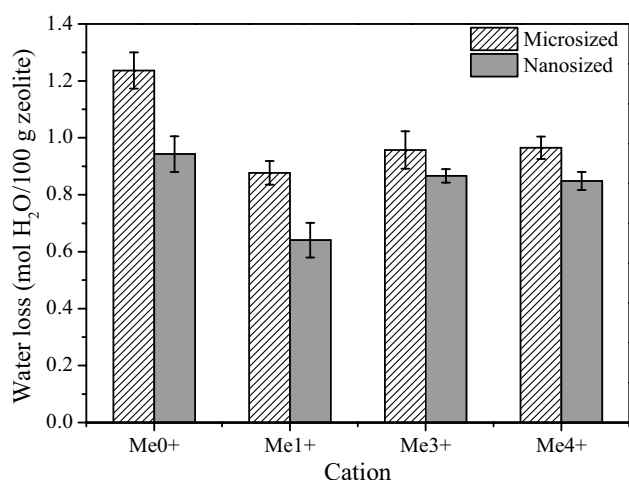


Fig. 9 Molar losses of water from the micrometric and nanometric zeolites containing methylammonium cations

weight losses between 200 and 800 °C (Regions II+III in Fig. 8). For most of the cations used, the nanometric zeolite had a higher content of organic cations, compared to the micrometric zeolite. These results agreed with the degree of exchange of sodium cations (Figs. 2, 3) and could be explained by the greater accessibility of the nanometric zeolite. In the case of the tetramethylammonium cation, Me₄⁺, the influence of accessibility was less pronounced because of its greater kinetic diameter, so the contents of this cation in the two zeolites were very similar.

3.5 Catalytic Evaluation

Figure 10 shows the conversions of butyraldehyde in the Knoevenagel condensation with ethyl cyanoacetate at 50 °C, using the nanometric and micrometric zeolites, according to the type of exchanger cation. The catalytic activity of the nanometric zeolite was always greater than that of the micrometric material, even when both were in the sodium form. One possible reason for the greater activity of the nanometric zeolite was the presence of smaller crystals and particles (values of 12 nm and 0.3 μm, respectively), compared to the micrometric catalyst (80 nm and

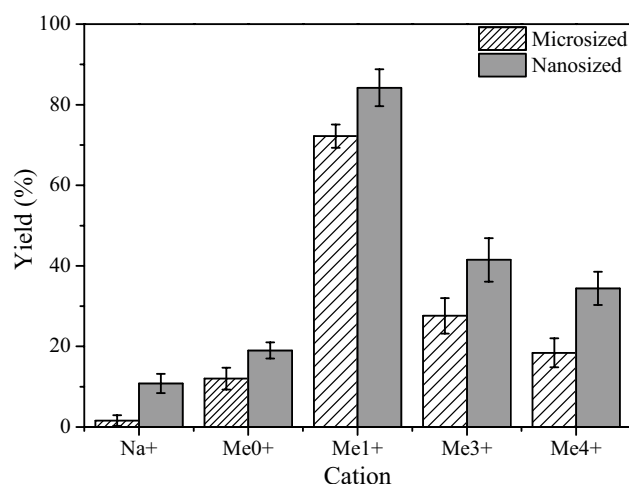


Fig. 10 Butyraldehyde conversions obtained using the nanometric and micrometric zeolites containing methylammonium cations (1 h, 50 °C and 3% w/w catalyst)

1–2 μm). The smaller crystallites and particles provided greater access to the catalytic sites due to more efficient diffusion of reactants and products through the zeolite pores. Another factor that could have contributed to the greater activity of the nanometric zeolite was the higher organic cation content of this material (Table 4) and consequently a greater number of catalytic sites (basic anions) [14].

It can also be seen from Fig. 10 that the catalytic activity of the faujasite was strongly dependent on the compensation cation. The lowest conversions were observed for the samples containing sodium cations, because Na⁺ had the smallest ionic radius, among the ions studied, and consequently produced catalytic sites with weaker basic properties.

Figure 11a, b shows the X-ray photoelectron spectroscopy results for line 1 s of the oxygen for the micrometric and nanometric zeolites containing sodium and methylammonium cations. The binding energy of the electrons with oxygen, E_b[O1s], is indirectly indicative of the basic strength. The lower the E_b[O1s] binding energy, the greater the ability to donate electrons, therefore the greater the Lewis basicity of oxygen.

The energy levels for the emission of the photoelectrons have a discrete distribution of energy, so the binding energy for the line 1 s of the oxygen will always have a value close to 531.5 eV [13, 29]. The Gaussian distribution of the O1s lines (Fig. 11) indicates the presence of only one oxygen species attributed to the structural oxygen of faujasite. Although all oxygen atoms are potential basic sites, only those belonging to the aluminate anions have sufficient basicity for catalytic activity [30].

The catalytic activity increased from 10 to 85% (Fig. 10) with increasing radius of the cation and decreasing acidity

Table 4 Contents of organic matter (mols Me_i⁺/100 g) in the micrometric and nanometric X zeolites (using heating from 200 to 800 °C)

| Cation | Micrometric | Nanometric | Δw (%) ^a |
|------------------------------|-------------|------------|---------------------|
| Me ₀ ⁺ | 63.4 | 73.2 | 15 |
| Me ₁ ⁺ | 44.0 | 52.0 | 18 |
| Me ₃ ⁺ | 18.0 | 21.2 | 18 |
| Me ₄ ⁺ | 11.8 | 11.4 | −3 |

^aDetermined by thermogravimetry, using: 100*(m_{nano}−m_{micro})/m_{micro}]

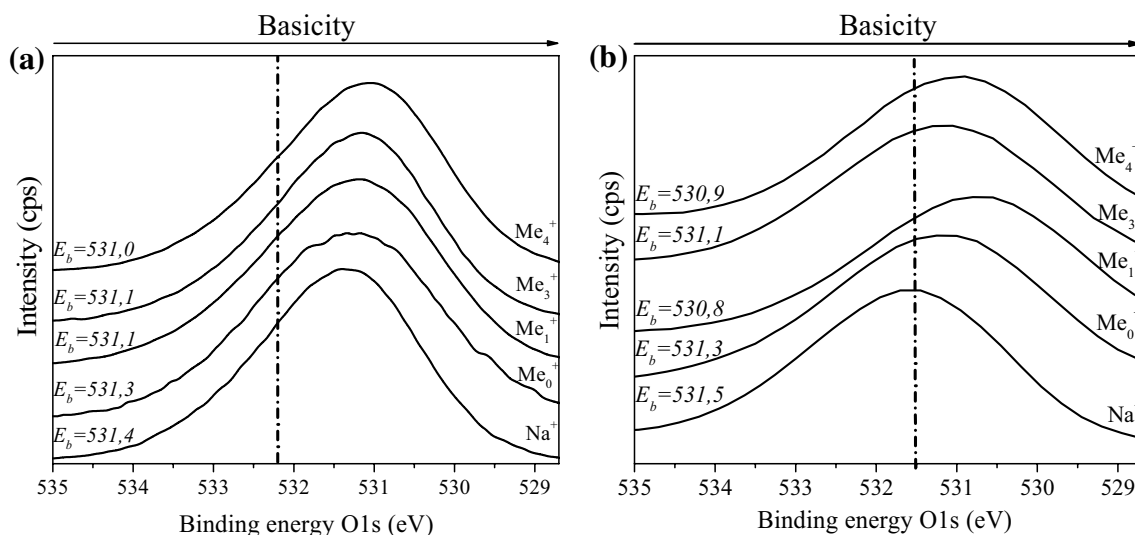


Fig. 11 XPS spectra for the micrometric (a) and nanometric (b) zeolites containing sodium (Na^+) and methylammonium cations (Me_i^+)

(Table 3), following the order $Na^+ < Me_0^+ < Me_1^+$, in this sequence also reduces the binding energy of line 1 s of the oxygen (Fig. 11). According to the Lewis acid-base model, the basicity of the conjugated anion increased in this order, in accordance with the catalytic activity. However, the conversions progressively decreased for zeolites exchanged using cations with radius greater than that of methylammonium, due to their greater volumes. These results show that although the basicity of the sites continued to increase, as demonstrated in Fig. 11, the catalytic activity decreased because it was strongly affected by steric hindrance, which restricted ion exchange and also impeded access of the reagents to the catalytic sites [11–13].

Since the Me_1^+ cation provided the best conversions, the reaction kinetics was studied in two temperatures (10–50 °C). The Fig. 12 shows the butyraldehyde

conversions versus time achieved using the nanometric and micrometric zeolites. Notice that for both temperatures studied, the microsized zeolite shows better conversions in relation to microsized from the first minutes of the reaction. Thus demonstrating that, reducing the size of the zeolite particles provides greater accessibility and diffusion of reactants and products by the pores of the catalyst. Besides, the conversions achieved at 10 °C in nanosized zeolite exceeded those obtained at 50 °C using the two zeolites containing the other cations.

The stability of the catalysts was assessed by means of four successive uses in the Knoevenagel condensation, under the conditions described above. Figure 13 shows the relationship between the butyraldehyde conversions obtained in the fourth and first uses (Eq. 2). The results showed that the catalytic stabilities of the nanometric and

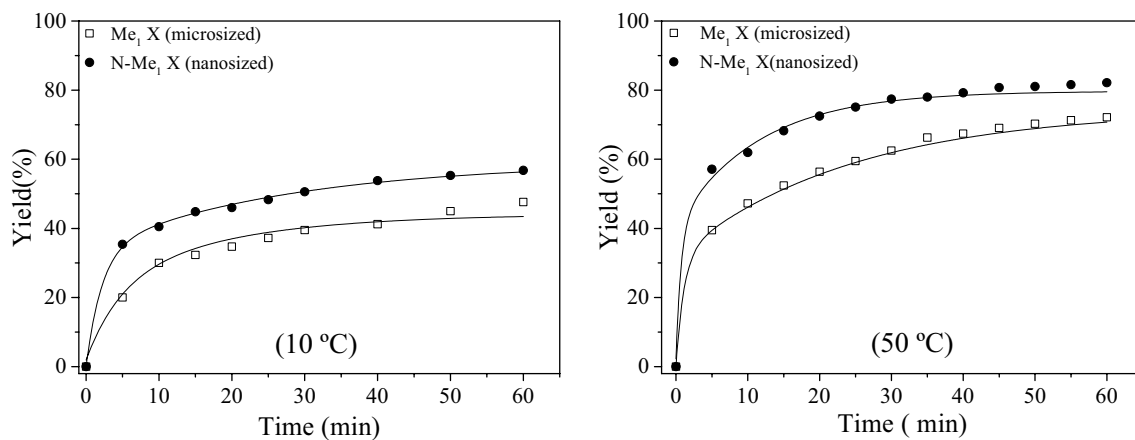


Fig. 12 Conversion versus time for Knoevenagel condensation of Me_1X and $N-Me_1X$ catalyst with different reaction temperature (3% w/w catalyst)

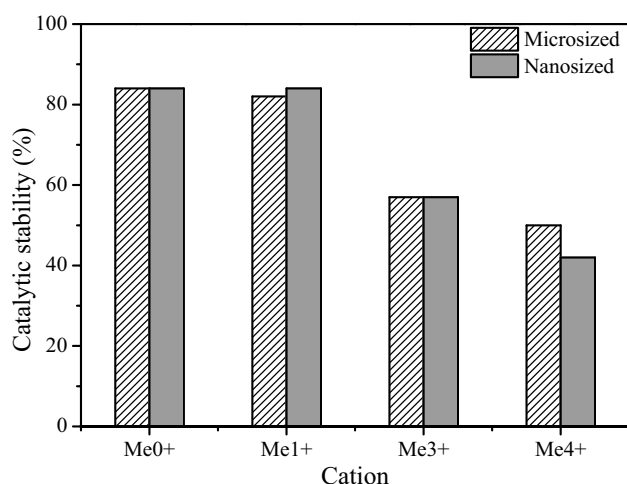


Fig. 13 Catalytic stability of the micrometric and nanometric zeolites (1 h, 50 °C and 3% w/w catalyst)

micrometric catalysts were very similar, irrespective of the cation volume. The catalysts containing the Me_0^+ and Me_1^+ cations presented good stability, with conversion maintained at 80% of the initial values after four uses. However, in the case of the bulkier cations (Me_3^+ and Me_4^+), there were greater decreases in catalytic activity during the four reuses. This could be attributed to the increased cation volume (above Me_1^+), which hindered the release of the products formed within the pores, hence restricting access to the catalytic sites [13]. This factor can be confirmed after thermogram analysis of the catalyst N- Me_4X without and after the fourth use (Figure S.4). After the fourth use the mass loss increased by 14%, which corresponds to the mass loss of the adsorbed product. In the thermogram analysis can be observed that the peak related to water loss became more intense and there is the presence of an additional peak in 218 °C, this refers to the decomposition of the product.

Table 5 shows the catalytic activity per site (TOF_0) for the catalysts exchanged with different cations, calculated from the derivative value of the curves showed in Fig. 12, at the beginning of the reaction ($t=0$). Considering the number of aluminum atoms per unit cell, the calculations assumed that the number of sites per gram of the type X FAU zeolite was equal to 4.57×10^{21} . It was also assumed that only the oxygen anions compensated by the different methylammonium or ammonium cations are associated with catalytic basic sites for this reaction (Table S.1) [9, 13].

The samples exchanged with Me_0^+ showed the lowest TOF values, which could be explained by the fact that this cation had the smallest ionic radius, among the cations tested, resulting in the generation of catalytic sites with weaker basic properties. For the samples exchanged with methylammonium cations, the TOF values decreased as

Table 5 Turnover frequencies (TOF) of the micrometric and nanometric zeolites exchanged using Me_i^+ cations (1 h, and 3% w/w catalyst)

| Cation | Reaction temperature (°C) | TOF (min^{-1}) | |
|-----------------|---------------------------|---------------------------|------------|
| | | Micrometric | Nanometric |
| Me_0^+ | 50 | 0.9 | 1.4 |
| Me_1^+ | 10 | 8.1 | 17.7 |
| Me_1^+ | 50 | 48.2 | 71.2 |
| Me_3^+ | 50 | 12.6 | 14.1 |
| Me_4^+ | 50 | 8.9 | 11.1 |

the cations became bulkier, with the greatest differences found comparing the Me_1^+ cation with the other cations.

These results showed that although the basicity of the sites increased with cation radius, the catalytic activity of the sites was strongly influenced by steric hindrance, which restricted ion exchange and impeded access of the reactants to the catalytic sites. As a result, higher TOF values were obtained for the nanometric zeolite.

The TOF of 48.2 min^{-1} obtained for the micrometric zeolite produced using the Me_1^+ cation and reaction temperature of 50 °C was close to the value of 49.7 min^{-1} reported by Almeida et al. [13] However, superior results were achieved with the nanometric catalyst, irrespective of the exchanger cation used. In the case of the Me_3^+ and Me_4^+ cations, although the basicity increased as a function of volume, the steric hindrances that limited ion exchange also restricted the catalytic activity per site, which led to lower TOF values [12, 29].

When the Me_1^+ cation was used, the best TOF values were once again achieved using the nanometric material produced using a temperature of 50 °C, for which the TOF value was nearly 50% higher than obtained with the micrometric material. The TOF obtained for the reaction at 10 °C was 17.7 min^{-1} .

The findings therefore demonstrated that greater accessibility and diffusion of reactants and products through the pores of the nanometric material acted to mitigate the limitations on the reaction resulting from the use of low temperatures. The N- Me_1X catalyst showed the best catalytic performance, which could be explained by the presence of basic sites that were more active due to the presence of the Me_1^+ cations, as well as greater access to the catalytic sites due to smaller sizes of the particles and the zeolite crystals.

4 Conclusions

The crystallization temperature used was found to be an important parameter in the synthesis of nanometric FAU

zeolite, with a crystalline product obtained in only 24 h at 60 °C, using only a single static phase synthesis. Preliminary catalytic evaluation showed that although the materials were synthesized in the sodium form, which is associated with low zeolite basicity, the small sizes of the crystals and particles provided greater access to catalytic sites and improved the diffusion of reactants and products through the pores of the nanoparticles, enabling better catalytic yields to be achieved.

The ionic exchange of sodium cations present in the X zeolite composed of micrometric particles was restricted to the supercavities, because the openings of the faces of the hexagonal prisms prevented exchange occurring in the interiors. As a result, the maximum exchange of sodium ions was limited to 81%. However, these restrictions were less important in the case of the nanometric zeolite particles, because the smaller dimensions of the particles increased access of the exchanger cations to the sodium ions located in the small cavities. This enabled degrees of sodium ion exchange up to 98% to be achieved.

In terms of catalytic activity, X zeolite containing monomethylammonium showed the best performance among the cations studied, indicating that there was an optimum relationship between the charge/radius ratio of the cation and the volume it occupied. The diminution of the particles to the nanometric scale improved the activity of the zeolites, due to the greater accessibility and better diffusion of reactants and products through the pores of the zeolite, leading to superior conversions. However, catalytic stability was not dependent on particle size, but decreased with increasing size of the compensation cation, due to deposition of the product within the pores. The greater accessibility and better diffusion of reactants and products through the pores of the zeolite with crystal and particle sizes of 12 and 300 nm, respectively, led to improved conversions and TOF, together with satisfactory catalytic stability.

Acknowledgements The authors are grateful to CNPq and CAPES for the financial support to this work, to Dr. Peter Hammer (Chemistry Institute, UNESP-Araraquara) for the XPS measurements.

References

- Morales-Pacheco P, Domínguez JM, Bucio L, Alvarez F, Sedran U, Falco M (2010) *Catal Today* 116:25
- Inagaki S, Thomas K, Clet G, Wakihara T, Shinoda S (2014) *ACS Catal* 4:2333
- Chaves TF, Pastore HO, Cardoso D (2012) *Microporous Mesoporous Mater* 67:161
- Bekkum HV, Flanigen EM, Jacobs PA, Jansen JC (2001) *Introduction to zeolite science and practice*. 2nd ed. Elsevier, Amsterdam
- Lind ML, Ghosh AK, Jawor A, Huang X, Hou W, Yang Y, Hoek EMV (2009) *Langmuir* 25:10139
- Tanabe K, Ho WFH (1999) *Appl Catal A*, 181(2):399
- Martins L, Cardoso D (2006) *Quim Nova* 29:358
- Valtchev V, Tosheva L (2013) *Chem Rev* 113:6734
- Theng BKG, Vansant E, Uytterhoeven JB (1968) *Trans Far Soc* 64:3370
- Barrer RM, Papadopoulos R, Rees LVC (1967) *J Inorg Nuclear Chem* 29:2047
- Martins L, Holderich W, Cardoso D (2008) *J Catal* 258:14
- Almeida KA, Martins L, Cardoso D (2010) *Quim Nova* 30:1077
- Almeida KA, Landers R, Cardoso D (2012) *J. Catal* 294:151
- Martins L, Boldo RT, Cardoso D (2007) *Microporous Mesoporous Mater* 98:166
- Colella C (1996) *Miner Dep* 31:554
- Lippens BC, De Bôer JH (1965) *J Catal* 4:319
- Li Q, Mihailova B, Creaser D, Sterte J (2001) *Chem Mater* 14:51
- Bo W, Hongzhu M (1998) *Microporous Mesoporous Mater* 10:1483
- Valtchev VP, Bozhilov KN (2004) *J Phys Chem* 108:15587
- Mintova S, Valtchev V (1999) *Stud Surf Sci Catal* 125:141
- Barthomeuf D (1984) *J Phys Chem* 88:42
- Wieland WS, Davis RJ, Garces JM (1996) *Catal Today* 28:443
- Lima PM, Gonçalves CV, Cavalcante Jr CL, Cardoso D (2008) *Microporous Mesoporous Mater* 116:352
- Breck DW (1974) *Zeolite molecular sieves*, Wiley, New York
- Nightingale ER (1959) *J Phys Chem* 63:1381
- Kresnawahjuesa O, Olson DH, Gorte RJ, Kühn GH (2002) *Microporous Mesoporous Mater* 51:175
- Pothen C, Francis GD (1980) *J Catal* 61, pp 452
- Hickson DA, Csicsery SM (1968) *J Catal* 10:27
- Almeida KA, Cardoso D (2013) *Catal Today* 213:122
- Barthomeuf D (2003) *Microporous Mesoporous Mater* 66:1